J Mater Sci (2011) 46:3464–3469
DOI 10.1007/s10853-011-5251-z

Study of the thermal properties of shape memory polyurethane nanofibrous nonwoven

Haitao Zhuo · Jinlian Hu · Shaojun Chen

Received: 16 November 2010 / Accepted: 6 January 2011 / Published online: 25 January 2011

Abstract Thermal properties of polymer are very important to the understanding of morphology and shape memory effect of shape memory polymers (SMPs). In this article, the thermal properties of shape memory polyurethane nanofibrous nonwoven are investigated systematically from the morphology of nanofibers, crystalline structure, isothermal crystallization behavior, and thermal-dependent strain recovery. The results indicate that the thermal properties of shape memory polyurethane nanofibrous nonwoven are influenced greatly by the electrospinning and the recrystalline condition. The crystal melting temperature (T_m) decreases as the crystallization temperature (T_c) decreases, while the relative degree of crystallinity (X_c) increases with the decrease of T_c within the temperature range of 20 to −30 °C. In particular, when the annealing temperature is higher than 150 °C, the T_m shifts to higher value and the X_c decreases significantly with the increase of T_c. Finally, temperature-dependent strain recovery curves show that the shape memory polyurethane nanofiber tends to have a lower recovery temperature as compared with the SMPU bulk film due to their ultrafine diameter.

Introduction

Shape memory materials (SMMs) are attractive because of their capability of changing their shapes upon exposure to an external stimulus like heat, pH, light, etc. [1–3]. The typical examples of SMMs include shape memory alloy [4], shape memory ceramics [5], and shape memory polymers (SMPs) [6, 7]. On the basis of the nature of switching segments, SMPs can be summarized into two main categories: T_m-type-SMPs with crystalline switching segment and T_g-type-SMPs with amorphous switching segment [1, 8]. The switching segments or soft phase and hard domains play the roles of reversible phase and fixed phase, respectively. As for the T_m-type-SMPs, high crystallinity in the soft phase at room temperature and the formation of hard domains above the crystal melting temperature (T_m) of soft phase are the two necessary conditions for segmented polymer exhibiting shape memory effect [9, 10]. As for the T_g-type-SMPs, the glass transition temperature (T_g) is designed to beyond ambient temperature. Accordingly, many glycols including PCL, PTMG, PHAG, and PBAG were used to synthesize polyurethane SMPs, named shape memory polyurethane (SMPU) [11].

In the previous literature [12–15], thermal properties were studied carefully as one of the main factors influencing shape memory properties of SMPU. For example, Kim et al. [12] studied the influence of block length and content on the thermal properties of T_g-type-SMPU systematically before investigating their thermal-induced shape memory behaviors. They found that the micro-phase separation was increased in the ionomers with high soft segment content according to the thermal properties of PCL-based SMPU ionomers and nonionomers [13]. Yang et al. [14, 15] studied the influence of carbon nanopowder and moisture on the T_g of T_g-type-SMPU before investigating their water-driven shape memory behaviors. Chen et al. [6, 16, 17] had also investigated systematically the effect of micro-phase separation promoter, molecular weight of polymer, hard segment content and soft segment length on the shape memory properties by combining with

H. Zhuo · J. Hu (✉) · S. Chen
Institute of Textiles and Clothing, The Hong Kong Polytechnic University, Hung Hom, Kowloon, Hong Kong, China
e-mail: tchujl@inet.polyu.edu.hk

the thermal properties of SMPU. These investigations support that there are close relationships between the thermal properties and the shape memory properties in the SMPU.

Recently, polymer nanofibers had drawn great interest in science and technology due to their typical unique properties like high specific surface area per unit, small diameter and low basis weight [18, 19]. As a fascinating fiber fabrication technique, electro-spinning had gained substantial academic attention. Most importantly, the technique brought the research of shape memory polymers (SMPs) into nano-scales field after SMPU nanofiber was firstly electrospun in 2005 [20–22]. In addition to good shape recovery, many unique properties like water vapor permeability (WVP) and acid-sensitivity were developed in the SMPU nanofibers [23]. However, the thermal properties of SMPU nanofiber had not been investigated systematically until now. Understanding the thermal properties is very important to the study of shape memory behavior of SMPU nanofiber. Therefore, a study of thermal properties of SMPU nanofibers is presented in this article.

Experimental part

Materials

PCL-based SMPU resin with number average molecular weight of 180,000 (Mn = 180,000), containing 75% soft segment content and 4,000 soft segment length, was synthesized by bulk polymerization method according to the procedure described in the earlier reports [6, 17]. In this experiment, the SMPU/DMF solutions with various concentrations for electro-spinning were obtained after the SMPU resin was dissolved into DMF at room temperature.

Electro-spinning

In this experiment, multiple nozzles were used to improve the electrified fluid jet speed in the electro-spinning. The multiple-nozzle electro-spinning apparatus consisting of five syringes is presented in Fig. 1. The electro-spinning process was carried out at room temperature. The solution flow rate was controlled to 0.08 mm/min by a syringe pump. The applied positive voltage was adjusted from 12 to 25 kV. The target consisted of a grounded aluminum sheet placed 15 cm from the needle tip to ensure that the fibers were dried upon collection.

Measurements and characterization

DSC was performed using a Perkin Elmer DSC. The samples (ca. 4 mg) were heated from −60 to 270 °C at a heating rate of 10 °C/min. After that they were kept at a constant temperature of 250 °C for 2 min and subsequently quenched to −60 °C. Finally, the first heating scan was repeated. The result of the second heating scan of each sample was used as a reference.

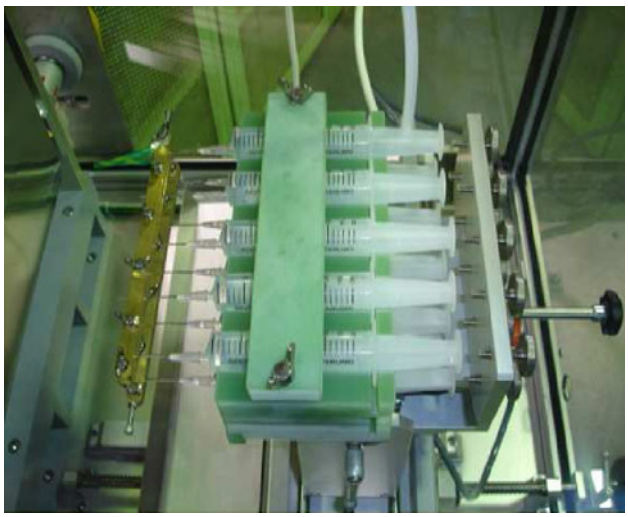

Fig. 1 Apparatus of multi-jet electro-spinning with a group of syringes and nozzles

Scanning electron microscope (SEM, Hitachi S450, Japan) was used to investigate the morphology of samples. Samples for SEM were obtained by spinning the nanofibers directly onto aluminum foil and gold-coated prior to SEM.

Thermal-strain recovery testing was performed in a microscopy (Leitz Wetzlar) with a hot stage (Mettler Toledo FP90 Central Processor & FP82 Hot Stage) and a camera (Pixera PVC 100C). The heating rate of strain recovery measurement was 2 °C/min, and the length of specimen was recorded on heating process within a temperature range from 25 to 100°C [9]. In addition, thermal-induced shape memory behaviors were also characterized with cyclic tensile test method according to the literature method [24]. The test was done using an instron 4466 apparatus with a temperature-controlled chamber, and a personal computer was used to control and record all data. The shape fixity and shape recovery were calculated from the recorded cyclic strain–stress curve.

Results and discussions

Morphology of nanofibers

Figure 2 shows the typical SEM images of SMPU nanofiber electro-spun from 10 wt% solution under the conditions of 20 kV applied voltage and 0.08 mm/min feeding rate. It is observed that the SMPU nanofibrous nonwoven is smooth, but not too uniform. The diameter of nanfibers is

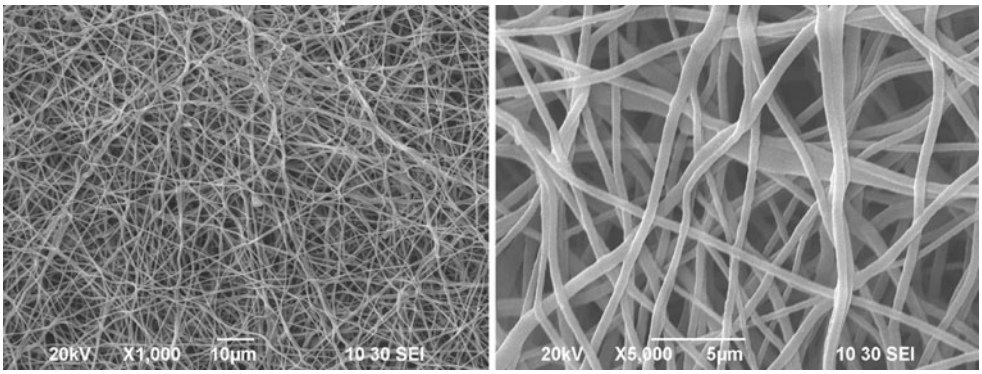

Fig. 2 SEM image of SMPU nanofibrous nonwoven by multi-electrospinning

changed from 600 to 700 nm. The thickness of nonwoven is increased layer-by-layer as the deposition time increases. As a result, interconnected fibrous network structures containing a lot of pores is formed in the resulted SMPU nanofibrous nonwoven. Moreover, there are no beads on the surface of SMPU nanofibers.

Figure 3 shows DSC curves of the nanofibrous nonwoven electrospun from 10 wt% solution under different applied voltage. In the earlier report [18, 19], it is known that the SMPU nanofiber show a different thermal properties because of their higher tropism structures as compared with its bulk film. Generally, the PCL-based SMPU nanofibrous nonwoven forms higher crystallinity structure while their micro-phase separation is poor. The T_m of electrospun fibres will decrease when higher concentration solution is used for electrospinning. Similarly, this micro-phase separation morphology with the crystalline soft phase and amorphous hard domain was confirmed by the DSC curves in Fig. 3. In addition, it can be found that the T_m of soft segment in the SMPU nanofibrous nonwoven increases with the increase of applied voltage, ranging from 40.4 to 43.2°C, on the heating curves. The recrystallization temperature (T_{rc}) increases with the increase of applied voltage on the cooling scans (not shown). It implies that the higher electrical force results in better tropism in the polymer chain of nanofiber. These results indicate that the thermal properties of SMPU nanofibrous nonwoven are influenced by the applied voltage and solution concentration.

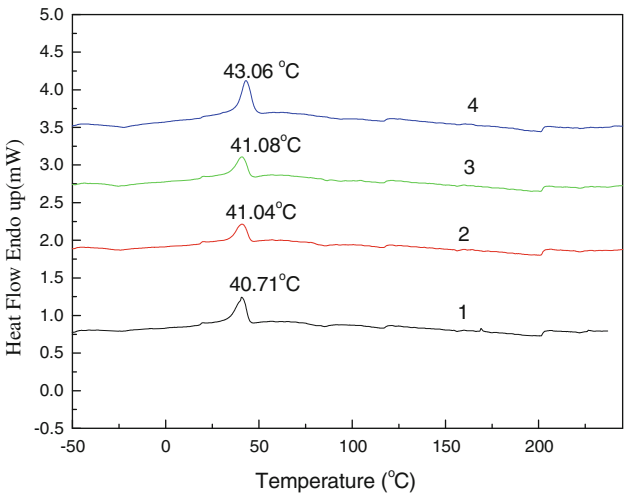

Fig. 3 DSC curves of nanofibrous nonwoven electrospun from different applied voltage (1–12 kv, 15 kv, 20 kv, 25 kv)

WAXD analysis

Figure 4 shows the WAXD profiles of SMPU nanofiber electropsun from different concentration solutions. In the earlier communication [18], it was known that the diameters of nanofiber were influenced greatly by the solution concentration. The diameters of SMPU nanofiber increased linearly with increasing the concentration. 50 to 100 nm nanofibers were prepared from 3.0 wt% solution, while 600–700 nm nanofibers were observed in the 12.0 wt% spun samples. Thus, the WAXD profiles of SMPU nanofiber electropsun from different concentration solutions show the influence of diameters on the crystalline behavior of SMPU nanofiber. In the previous literature [17], it was observed that the PCL-based SMPU bulk film have two prominent peaks at Bragg angles of 21.41° [100] and 23.74° [101], indicating the crystalline PCL soft segment. The pattern also features one broad peak from 20.56° to 20.97°, suggesting the presence of an amorphous structure in their soft phase. In this experiment, the SMPU nanofiber nonwoven was electro-spun from the PCL-based SMPU/DMF solution. Thus, there are also two prominent peaks at Bragg angles of 21.36° [100] and 23.65° [101] in Fig. 4. However, there are no big differences among different SMPU nanofiber nonwoven though they contain different diameters nanofiber. As compared with the WAXD profiles of SMPU bulk film in literature [17], the broad peak featuring the amorphous soft phase is very weak in the SMPU nanofiber nonwoven. These results imply that all the SMPU nanofiber nonwovens have the excellent

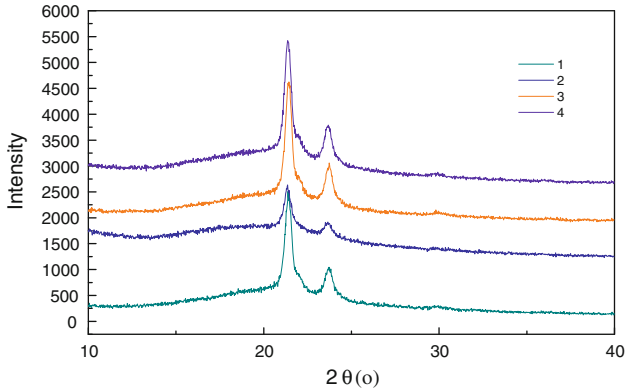

Fig. 4 WAXD profiles of SMPU nanofiber electropun from different concentrations (1–5 wt%; 2–7 wt%; 3–10 wt%; 4–12 wt%)

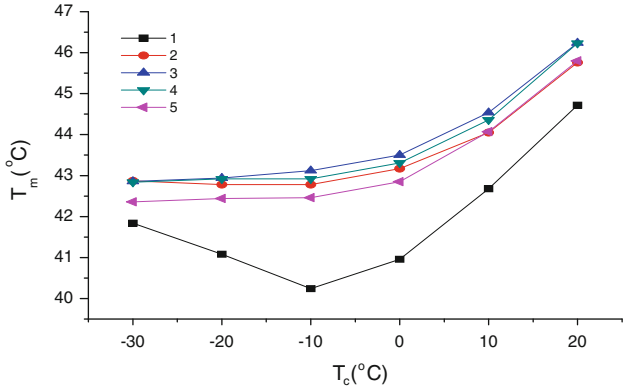

Fig. 5 Dependency of T_m on T_c in various nanofibrous membrane electrospun from different concentrations (2–12 wt%; 3–10 wt%; 4–7 wt%; 5–5 wt %) as compared with the bulk film (*1*)

crystallizability in the soft phase; and the SMPU nanofiber nonwovens show higher relative crystallinity.

Isothermal crystallization

To further investigate the crystalline behavior of SMPU nanofiber, isothermal crystallization experiments were performed with a Perkin-Elemer diamond differential scanning calorimeter in this experiment. During the testing process, the sample was initially heated to a temperature above T_m, e.g., 70 °C, at a rate of 10 °C/min and held at this temperature for 5 min to melt the crystalline soft phase. It was then rapidly (60 °C/min) cooled down to a designated crystallization temperature (T_c), and held at this temperature to the end of the exothermic crystallization [25]. On the second heating curves, the T_m of soft phase and their enthalpy datum (ΔH_m) were recorded for the analysis of thermal properties. The degree of relatively crystallinity (X_c) was calculated from the ΔH_m by using an reference enthalpy value for fusion of 100% crystalline PCL, 136.5 J/g of the heat fusion given by Crescenzi et al. [17]. Finally, the dependency of T_m and X_c of soft segment on the T_c can be drawn as shown in Figs. 5 and 6.

In Fig. 5, it can be found that all the SMPU nanofiber nonwovens show the similar T_m change tendency with respect to the change of T_c, i.e., the T_m of soft segment shifts to lower temperature as the T_c decreases from 20 to −10 °C, and it tends to keep a stable value below −10 °C. However, the SMPU bulk film shows the lowest T_m after it is crystallized at −10 °C. The T_m also increases as the T_c increases from −10 to 20 °C, and it increases as the T_c decreases from −10 to −30 °C. At the same time, it is found in Fig. 6 that the X_c of SMPU nanofiber nonwoven decreases significantly with the increase of T_c. It means that a lower crystallization temperature will improve the X_c of soft phase greatly. For example, the X_c increases from 16 to 26.6%, when the T_c decreases from 20 to −30 °C.

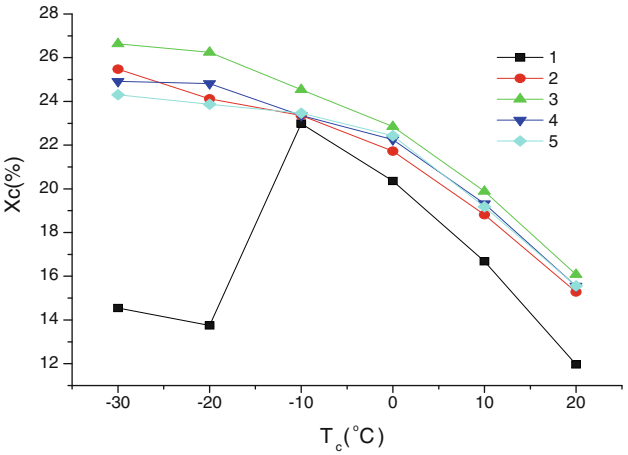

Fig. 6 Dependency of X_c on T_c in various nanofibrous nonwoven spun from different concentrations (2–12 wt%; 3–10 wt%; 4–7 wt%; 5–5 wt%) as compared with bulk film (*1*)

However, the maximum value of X_c of bulk film is observed in the sample crystallized at −10 °C. Its X_c decreases with the increase of T_c above −10 °C as well as the decrease of T_c below −10 °C. This is due to the fact that high orientation structure is formed while the micro-phase separation is not very good in the nanofiber as compared with the bulk film. The poor phase separation influences the formation of soft segment crystal at higher T_c condition. A lower T_c promotes the formation of crystal of soft segment due to the higher orientation structure in the electrospun nanofiber. However, the formed crystal at higher T_c tends to be more stable as compared with those formed at lower T_c, since the soft segment is oriented in the electrospun nanofibers.

In the practical application, annealing temperature generally influences the thermal properties of SMPU greatly. In this experiment, the SMPU nanofiber was firstly

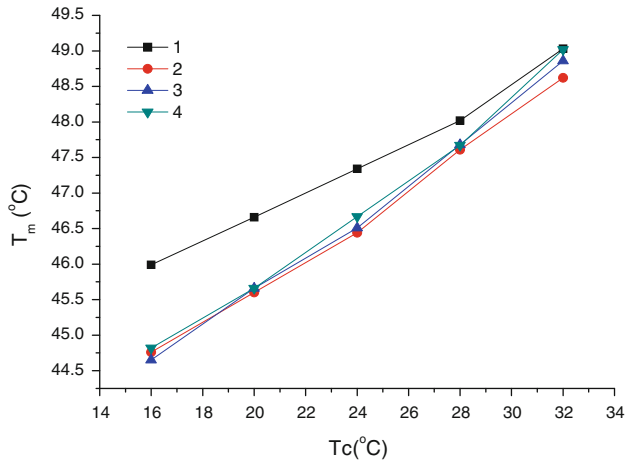

Fig. 7 Dependency of T_m on T_c of nanofiber after different annealing temperatures (1–150 °C; 2–120 °C; 3–100 °C; 4–70 °C)

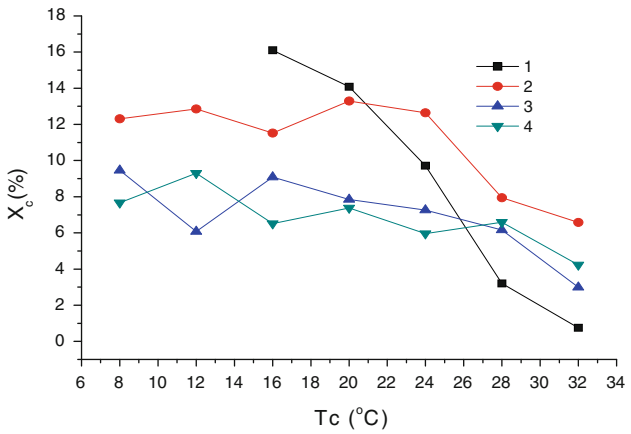

Fig. 8 Dependency of X_c on T_c of nanofiber after different annealing temperatures (1–150 °C; 2–120 °C; 3–100 °C; 4–70 °C)

heated to a designed annealing temperature like 70, 100, 120, and 150 °C. They were then cooled down to the designed T_c, concentrating on the temperature range of 16 to 32 °C. Finally, the dependency of T_m and X_c on T_c of nanofiber through different annealing temperatures can be obtained as shown in Figs. 7 and 8, respectively. In Fig. 7, it is observed that the T_m increases lineally with the increase of T_c in all SMPU nanofiber nonwovens as mentioned above. This result is very consistent with the observation of temperature memory by Poulin [26]. They reported that the strain recovery and the stress generation appeared at the temperature of their initial deformation in the T_g-type-SMP. In addition, it is well known that the strain recovery of T_m-type-SMPU is trigged by the crystalline soft phase, and the T_m is very close to the strain recovery temperature. Thus, this result implies that the SMPU nanofiber tends to have a lower strain recovery temperature, if the deformed strain is fixed at a lower crystallization temperature. This is due to the fact that the crystals formed at lower T_c condition tend to be unstable as compared with the crystals formed at higher T_c condition. It is worth noting that the T_m changes little at any T_c when the annealing temperature is below 120 °C. However, it shifts to higher temperature range when the annealing temperature is 150 °C. This is due to the fact that the hard domains are destroyed above 150 °C and the micro-phase separation structure is reassembled after it is cooled down to the T_c. In addition, it is also found in Fig. 8 that the X_c decreases significantly with the increase of T_c, when the sample is annealed above 150 °C. For example, the X_c decreases from 16.3 to only 0.83% as the T_c increases from 16 to 32 °C after the SMPU nanofibers is annealed above 150 °C. However, it changes a little by varying the T_c if the annealing temperature is below 120 °C; and the sample tends to have the maximum X_c after an annealing process at 120 °C. It implies that the initial morphology and high tropism structure of nanofiber is kept below 120 °C. A higher annealing temperature tends to show a higher X_c if the nanofiber structure does not destroyed.

Temperature-dependent strain recovery property

Thermal recovery testing is widely used to characterize the temperature-dependent shape recovery behaviors [27]. Figure 9 presents the temperature-dependent strain recovery curves of SMPU nanofiber nonwovens. It is found that all the samples including bulk film and SMPU nanofiber nonwovens show the typical S-shaped temperature-dependent strain recovery curves, i.e., the sample tends keep their original shape before the temperature is raised to above its shape recovery started temperature. It then recovers abruptly within a short temperature range. Finally, the length is changed slowly to a relative stable value, closing to their original length. In the temperature-dependent shape recovery curves, not only the strain recovery started temperature, but also the strain recovery temperature at which 50% deformed strain is recovered can be found. For example, the strain recovery temperatures of SMPU nanofibers electrospun from 5 and 7 wt% solution are 49 and 43 °C, respectively. It shows that the strain recovery temperature is relatively high in the lower concentration solution. This is due to the fact that the electrospun nanofibers from the lower concentration solution tend to have smaller diameters but higher molecular orientation, resulting in more stable crystals in the soft phase. It is worth noting that the bulk film generally shows the higher strain recovery temperature as compared with the nanofibers nonwoven though their DSC curves show a higher T_m in the nanofiber. This is due to the fact that the nanofibers have a very small diameter and their nonwoven contains lots of pores. This structure shows fast response to the

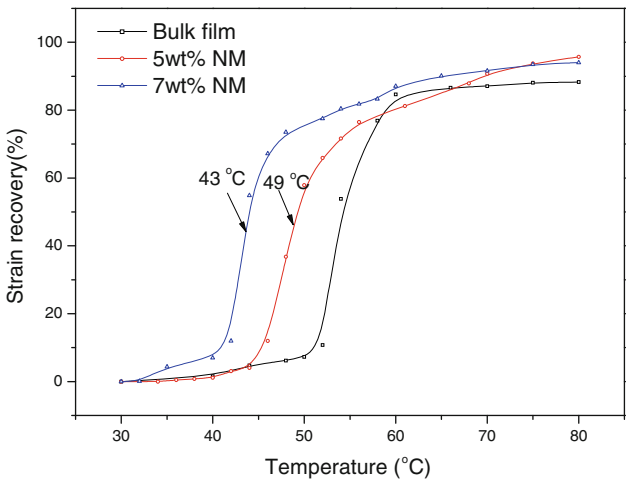

Fig. 9 Strain recovery curves of SMPU nanofiber membrane electrospun from different concentrations (5 and 7 wt%) as compared with bulk film

stimulus of heat. Thus, the deformed strain of SMPU nanofibrous nonwoven is recovered at a lower temperature quickly. As for the final strain recovery, it is also found in Fig. 9 that the SMPU nanofibers still have the higher maximum strain recovery as compared with bulk film. This result is very consistent with the result of thermal-mechanical testing as reported before. It was reported that the SMPU nanofiber deposited nonwoven showed more than 98% shape recovery and about 80% shape fixity [18, 19].

Conclusions

In this article, the thermal properties of SMPU nanofibrous nonwoven are investigated systematically. Finally, the following conclusions can be summarized.

(1) The thermal properties of SMPU nanofibrous nonwoven are influenced by the applied voltage and solution concentration.

(2) Isothermal crystallization testing shows that the T_m of SMPU nanofiber decreases to a relative stable value as the T_c decreases, while the X_c increases with the decrease of T_c in the temperature range of -30 to 20 °C. However, the minimum T_m and maximum X_c in the bulk film are found in the sample crystallized at -10 °C.

(3) When the annealing temperature is higher than 150 °C, the T_m increases with the increase of T_c at any annealing temperature, while the X_c decreases significantly with the increase of T_c.

(4) Finally, the temperature-dependent strain recovery curves show that the SMPU nanofiber tends to have a relative lower recovery temperature as compared with the bulk film.

Acknowledgements This work was financially supported by the project G-T881 and PhD studentship of Hong Kong Polytechnic University. The authors wish to express their gratitude for the generous support.

References

1. Behl M, Lendlein A (2007) Mater Today 10:20
2. Chen SJ, Hu JL, Yuen CW, Chan LK (2009) Polymer 50:4424
3. Chen SJ, Hu JL, Zhuo HT, Yuen CW, Chan LK (2010) Polymer 51:240
4. Wang ZG, Zu XT, Zhu S, Wang LM (2005) Mater Lett 59:491
5. Schurch KE, Ashbee KHG (1977) Nature 266:706
6. Chen SJ, Hu JL, Liu YQ, Liem HM, Zhu Y, Liu YJ (2007) J Polym Sci 45:444
7. Chen SJ, Hu JL, Zhuo HT, Zhu Y (2008) Mater Lett 62:4088
8. Ratna D, Karger-Kocsis J (2008) J Mater Sci 43:254. doi:10.1007/s10853-007-2176-7
9. Cao Q, Chen SJ, Hu JL, Liu PS (2007) J Appl Polym Sci 106:993
10. Chen SJ, Cao Q, Liu PS (2006) Acta Polym Sin 1:1
11. Chen SJ, Hu JL, Yuen CW, Chan LK, Zhuo HT (2010) Polym Adv Technol 21:377–380
12. Kim BK, Shin YJ, Cho SM, Jeong HM (2000) J Polym Sci 38:2652
13. Kim BK, Lee SY, Lee JS, Baek SH, Choi YJ, Lee JO, Xu M (1998) Polymer 39:2803
14. Yang B, Huang WM, Li C, Li L, Chor JH (2005) Scr Mater 53:105
15. Yang B, Huang WM, Li C, Chor JH (2005) Eur Polym J 41:1123
16. Chen SJ, Cao Q, Jing B, Cai YL, Liu PS, Hu JL (2006) J Appl Polym Sci 102:5224
17. Chen SJ, Hu JL, Liu YQ, Liem HM, Zhu Y, Meng QH (2007) Polym Int 56:1128
18. Zhuo HT, Hu JL, Chen SJ, Yeung LP (2008) J Appl Polym Sci 109:406
19. Zhuo HT, Hu JL, Chen SJ (2008) Mater Lett 62:2078
20. Jung YC, Kim JW, Chun BC, Chung YC, Cho JW (2004) Qual Text Qual Life 1–4:43
21. So JH, Lee SH, Jung J, Yoon KJ, Cho JW (2004) Qual Text Qual Life 1–4:121
22. Cha DI, Kim HY, Lee KH, Jung YC, Cho JW, Chun BC (2005) J Appl Polym Sci 96:460
23. Zhuo HT, Hu JL, Chen SJ, Zhu Y (2008) In: Proceedings of the international conference on advanced textile materials & manufacturing technology, p 463
24. Chen SJ, Hu JL, Yuen CW, Chan LK (2009) Mater Lett 63:1462
25. Zhu Y, Hu JL, Choi KF, Meng QH, Chen SJ, Yeung KW (2008) Polym Adv Technol 19:328
26. Miaudet P, Derre A, Maugey M, Zakri C, Piccione PM, Inoubli R, Poulin P (2007) Science 318:1294
27. Li FK, Hou JN, Zhu W, Zhang X, Xu M, Luo XL, Ma DZ, Kim BK (1996) J Appl Polym Sci 62:631